Journal of Bioenergetics and Biomembranes, Vol. 34, No. 1, February 2002 (© 2002)

Iron-Induced Oxidant Stress in Nonparenchymal Liver Cells: Mitochondrial Derangement and Fibrosis in Acutely Iron-Dosed Gerbils and Its Prevention by Silybin

Antonello Pietrangelo,[1,3] Giuliana Montosi,[1] Cinzia Garuti,[1] Miranda Contri,[2] Fabiola Giovannini,[2] Daniela Ceccarelli,[2] and Alberto Masini[2]

Received December 21, 2001; accepted July 13, 2001

Hepatic fibrosis due to iron overload is mediated by oxidant stress. The basic mechanisms underlying this process in vivo are still little understood. Acutely iron-dosed gerbils were assayed for lobular accumulation of hepatic lipid peroxidation by-products, oxidant-stress gene response, mitochondrial energy-dependent functions, and fibrogenesis. Iron overload in nonparenchymal cells caused an activation of hepatic stellate cells and fibrogenesis. Oxidant-stress gene response and accumulation of malondialdehyde–protein adducts were restricted to iron-filled nonparenchymal cells, sparing nearby hepatocytes. Concomitantly, a significant rise in the mitochondrial desferrioxamine-chelatable iron pool associated with the impairment of mitochondrial oxidative metabolism and the hepatic ATP decrease, was detected. *Ultrastructural mitochondrial alterations were observed only in nonparenchymal cells. All biochemical and functional derangements were hindered by in vivo silybin administration which blocked completely fibrogenesis. Iron-induced oxidant stress in nonparenchymal cells appeared to bring about irreversible mitochondrial derangement associated with the onset of hepatic fibrosis.*

KEY WORDS: Iron; Kupffer cells; oxidative stress; mitochondrial dysfunction; fibrogenesis; gerbil.

INTRODUCTION

Hepatic fibrosis is regarded as a common response of the liver to a chronic insult which, regardless of its nature (e.g., viral infection, alcohol abuse, metal overload), leads to cell damage and/or necrosis followed by excessive deposition of extracellular matrix components (ECM) (Friedman, 1993). Thus, injury to hepatocytes can result in the recruitment and activation of inflammatory and macrophagic cells, including Kupffer cells. The resulting inflammatory cascade will lead to activation and proliferation of fibroblasts or fibroblast-like cells, such as the hepatic stellate cells (HSC) (formerly known as Ito cells or lipocytes) and a marked increase in their production of ECM. However, the hypothesis that additional pathways leading to hepatic fibrosis may operate during metal overload disorders is not unrealistic. For instance, early fibrogenesis in the absence of necro-inflammatory phenomena during iron overload disorders has been reported (Weintraub *et al.*, 1988). Yet, emerging experimental evidence supports independent stimulation of collagen gene expression at a "pre-necrotic" stage during oxidative-stress associated liver injury (Pietrangelo, 1996).

In the gerbil model of liver fibrogenesis, iron acts as a "co-factor" of fibrogenesis (Pietrangelo, 1996). It accumulates predominantly into nonparenchymal cell aggregates of preexisting gut-endotoxin induced lesions, leading to hepatic collagen deposition and progression toward hepatic cirrhosis within 6–12 weeks (Carthew *et al.*, 1991). Interestingly, in this model, hepatic fibrosis occurs in the absence of accompanying necrogenic events. We have recently shown that the molecular basis for this process is a fibrogenic and mitogenic effect exerted by hepatic iron

[1] Dipartimento di Medicina Interna e Sezione di Patologia Generale, Università di Modena, Modena, Italy.
[2] Dipartimento di Scienze Biomediche, Università di Modena, Modena, Italy.
[3] To whom correspondence should be addressed; e-mail: pietra@unimo.it.

0145-479X/02/0200-0067/0 © 2002 Plenum Publishing Corporation

overload on HSC (Pietrangelo *et al.*, 1995a). Although the driving force to fibrogenesis in the gerbil model of iron toxicity is represented by tissue iron load, the cellular basis for the events leading to micronodular cirrhosis in the absence of necrosis, is still unclear. In a recent study on chronically iron-treated gerbils we showed that irreversible oxidative anomalies of liver mitochondria accompanies with iron-induced fibrogenesis in the liver and this is partially prevented by a potent antioxidant (i.e. silybin) (Masini *et al.*, 2000). In the present study, by using in situ detection of oxidant stress gene response, membrane oxidation by-products and electron microscopy, we show that, in acutely iron-dosed gerbil, iron-induced oxidant stress is mainly localized in iron-loaded nonparenchymal cells and accompanies irreversible mitochondrial dysfunctions. Complete prevention of oxidant stress and mitochondrial defects by in vivo administration of silybin halts the expansion of nonparenchymal cell population and blocks fibrogenesis.

METHODS

Animals

Male gerbils (6 weeks of age) were housed in stainless steel cages and divided into four groups: *group A*: gerbils subcutaneously dosed with a single injection of iron–dextran (1 mg/g body wt) ($n = 12$); *group B*: gerbils subcutaneously dosed with 1 mg/g body wt of dextran alone ($n = 12$); *group C*; gerbils subcutaneously dosed with 1 mg/g body wt of iron–dextran and treated by gavage with 100 mg/kg body wt/day silybin (740 mg silybin-β-cyclodestrin complex/kg body wt/day) suspended in 10% acacia solution for 8 weeks ($n = 12$); *group D*: gerbils subcutaneously dosed with 1 mg/g body wt of dextran alone and treated by gavage with 100 mg/kg body wt/day silybin for 8 weeks ($n = 12$). A further group of animals was gavaged with the vehicle used to administer silybin (i.e. 10% acacia solution). Iron treated and control animals fasting overnight were killed by cervical dislocation after 8 weeks, the livers were rapidly removed and used for morphological, immunohistochemical, biochemical, and functional studies.

Light Microscopy

Thin liver slices were fixed in a 4% solution of paraformaldehyde in 0.1 mol/L phosphate buffer (PBS) pH 7.4, and embedded in paraffin. Five micrometer sections were cut and stained with hematoxylin and eosin, Mallory and Perls' Prussian blue.

Electron Microscopy

Fragments of the hepatic tissue were processed using standard procedures. They were fixed in 2.5% glutaraldehyde in Tyrode's solution pH 7.2, postfixed in 1% osmium tetroxide (OsO_4) in the same buffer, dehydrated in graded ethanols, and embedded in Spurr resin (Polyscience Inc. Warrington, PA, USA). Ultrathin sections were stained with uranyl acetate and lead citrate and examined with JEOL 1200 EX II electron microscope.

In Situ Hybridization and Generation of ^{35}S-Labeled RNA Probes

In situ hybridization analysis was performed on liver tissue frozen in liquid nitrogen and stored at -80°C. A *Eco*RI–*Hin*dIII 1300-bp fragment of rat pro-α_1(I) collagen cDNA (Genovese *et al.*, 1984) was subcloned in pGEM1 plasmid whereas as *Hin*dIII–*Eco*RI 883-bp fragment of the rat heme oxygenase-1 (HO-1) probe was subcloned in the pGEM blue plasmid (Shibahara *et al.*, 1985). To generate run-off transcripts of the antisense or sense strands, respectively, 1 μg of collagen plasmid was linearized with either *Hin*dIII or *Eco*RI restriction endonucleases and transcribed in vitro with 10 Units of T7 or SP6 RNA polymerases as reported (Pietrangelo *et al.*, 1995a). For the HO-1 plasmid, T7 and SP6 RNA polymerases were used to generate the sense and antisense run-off transcripts, respectively. Prehybridization, hybridization, and washing procedures were performed as previously described (Pietrangelo *et al.*, 1995a). After development in Kodak D19 developer and fixation in Kodak Fixer, the slides were counterstained with H & E, mounted, and viewed under light microscope in dark or bright field. The pro α_1(1)-collagen and the heme oxygenase-1 probes were generous gifts of C. Genovese (Farmington, CO, USA) and L. Tacchini (Milan, Italy), respectively.

Immunocytochemistry

Seven micrometer sections from frozen liver specimens were collected onto clean slides, treated as specified for the in situ hybridization analysis, fixed with a 4% solution of paraformaldehyde in 0.1 mol/L phosphate buffer (PBS) pH 7.4, washed twice with PBS, and incubated with the first antibody diluted 1:200 in solution A (10% fetal bovine serum in RPMI 1640): mouse monoclonal anti-human desmin (D33, Dakopatts, Glostrup, Denmark); monospecific antisera to malondialdehyde–lysine adducts (MAL-2), kindly provided by J. L. Witztum (University of California, San Diego) (Houglum *et al.*, 1990). Control

slides were incubated with solution A alone. All incubation steps were carried out as specified (Pietrangelo *et al.*, 1995b).

Preparation of Mitochondrial Fraction

A portion of the liver was used for preparation of mitochondrial fraction in 0.25 M sucrose according to a standard procedure (Masini *et al.*, 1983). The method provided a mitochondrial preparation whose cytosolic contamination did not exceed 2% of the total protein content as measured by recovery of marker enzymes (Botti *et al.*, 1989). Protein concentration was determined by the biuret method with bovine serum albumin as a standard.

Lipid Peroxidation

Thiobarbituric acid reactive substances (TBARS) in the mitochondrial fraction, as index of malondialdehyde (MDA) accumulation, were measured by the thiobarbituric acid method in the presence of 0.1% (w/v) butylated hydroxytoluene and 0.5 mM $FeCl_3$ added to the sample immediately before the addition of the thiobarbituric acid mixture (Tangeras, 1983).

Oxygen Consumption

Unless otherwise indicate, the standard incubation medium had the following composition: 100 mM NaCl; 5 mM sodium–potassium phosphate buffer (pH 7.4); 10 mM Tris-HCl buffer (pH 7.4); 10 mM $MgCl_2$. The respiratory substrates used were 2.0 mM potassium glutamate plus 0.5 mM potassium malate and 2.0 mM potassium succinate plus 4 μM rotenone. Oxygen uptake was measured with a Clark type oxygen electrode at 25°C in a final volume of 1 mL; mitochondrial concentration was 2 mg protein per vessel. The respiratory states were those defined by Chance and Williams on the basis of the factors limiting the respiratory rate (Chance and Williams, 1956).

Transmembrane Electrical Potential

The transmembrane electrical potential ($\Delta\psi$) was measured at 25°C, in a final volume of 1 mL of the same incubation medium used for respiratory assays, containing 16 μM tetraphenylphosphonium chloride (TPP^+), by monitoring with a TPP^+ selective electrode, the movements of TPP^+ across the membrane according to Kamo *et al.* (Kamo *et al.*, 1979).

Mitochondrial Desferrioxamine (DFO) Chelatable Iron

Mitochondrial DFO-chelatable iron concentration was measured as desdferrioxamine–iron complex (DFO) as previously described (Ferrali *et al.*, 1989). Briefly, mitochondrial samples (60–90 mg protein/mL) containing 25 μM desferrioxamine were lysed by freezing and thawing. Mitochondria were centrifuged at $100.000 \times g$ for 30 min. The supernatant was ultrafiltered by membrane cones (Centriflo CF 25, Amicon). The DFO-iron content of the aproteic ultrafiltrates was measured by an HPLC method (Kruck *et al.*, 1985).

Total Iron Determination

Iron content in samples from liver tissue and mitochondrial fraction was analyzed by atomic absorption spectroscopy, as previously reported (Cairo *et al.*, 1989).

Enzyme Assays

Succinate dehydrogenase and cytochrome oxidase activity was measured polarographically in freeze-thawed mitochondria as described in (Moreno and Madeira, 1991) at pH 7.4 and 25°C. Unless otherwise stated, 0.3 mg of Lubrol/mg protein were present in the incubation medium (Muscatello and Carafoli, 1969). Succinate:cytochrome *c* reductase activity was determined spectrophotometrically at 550 nm in freeze-thawed mitochondria (pH 7.4, 25°C) as described (Tisdale, 1967). Rotenone-sensitive NADH:cytochrome *c* reductase activity was determined spectrophotometrically at 550 nm in freeze-thawed mitochondria (pH 7.4, 25°C) as described (Hafety and Stiggal, 1978). After a measurable linear rate was observed, 2.5 μM rotenone was introduced to the assay to obtain a rotenone-insensitive rate. The rotenone-sensitive NADH:cytochrome *c* reductase rate was calculated by subtracting the rotenone-insensitive rate from the overall rate.

Serum Aminotransferases

Serum aminotransferases were measured by standard automated laboratory methods.

Measurement of Hepatic Adenosine Triphosphate

Adenosine triphosphate was measured in freeze-clamped liver by HPLC analyses as described (Pietrangelo *et al.*, 1995c).

Table I. Liver Total Iron, Weight Parameters, and Serum ALT Activities in Various Experimental Groups

Experimental condition	Total iron (μg/g wet wt)	Body weight (g)	Liver weight (g)	ALT (U/L)
Control	312 ± 46	63 ± 7	1.3 ± 0.2	78 ± 16
Iron	$5709 \pm 260^*$	60 ± 5	1.4 ± 0.2	64 ± 18
Silybin	320 ± 50	64 ± 6	1.3 ± 0.3	75 ± 20
Iron + silybin	$5885 \pm 310^*$	65 ± 7	1.5 ± 0.2	86 ± 12

Note. Total iron and ALT analyses were performed as described in Materials and Methods. Data are expressed as mean $\pm$ SD of three experiments performed on a pool of four animals.
$^*P < 0.01$ in comparison with control.

Statistical Analyses

All data in Tables I, II, and III are mean $\pm$ SD. Differences between iron-treated gerbils and the control counterpart (i.e. untreated gerbils on the standard diet, group B) were analyzed by the Student's *t* test.

RESULTS

The hepatic total iron content of acutely iron-treated gerbils appeared significantly increased as compared with control (Table I). No significant modification was observed when silybin was contemporary administered with iron. The body weight and the liver weight were not appreciably modified by iron treatment. As already reported (Carthew *et al.*, 1991; Pietrangelo *et al.*, 1995a), no cell damage appeared to be induced by iron treatment as also documented by unchanged serum aminotransferase levels (Table I).

Iron Overload and Liver Fibrogenesis

Iron-dosed gerbils developed hepatic fibrosis, as originally described by Carthew *et al.* (1991). In gerbils, iron overload of preexisting hemorragic necrotic foci caused a marked proliferation of nonparenchymal cells, including Kupffer cells, and accumulation of collagen (Pietrangelo *et al.*, 1995a). Iron treatment brought about a significant increase in the hepatic stellate cell number (HSC) (reddish colour) which surrounded hepatocyte nodules after 8 weeks from iron dosing (Fig. 2(B)). Non-immune serum showed no staining of HSC (Fig. 2(D)). By in situ hybridization for collagen mRNA, a strong activation was detected in liver nonparenchymal cells invading fibrous tissue bundles (Fig. 2(E)). Upon iron treatment, massive iron accumulation occurred in Kupffer cells and significant fibrosis developed after 8 weeks with appearance of typical nodularity (Fig. 1(B)) as compared with control (Fig. 1(A)). Silybin treatment decreased collagen gene expression which remained limited to preexisting necrotic iron-loaded microfoci (Fig. 2(F)), it also completely prevented collagen accumulation and preserved a

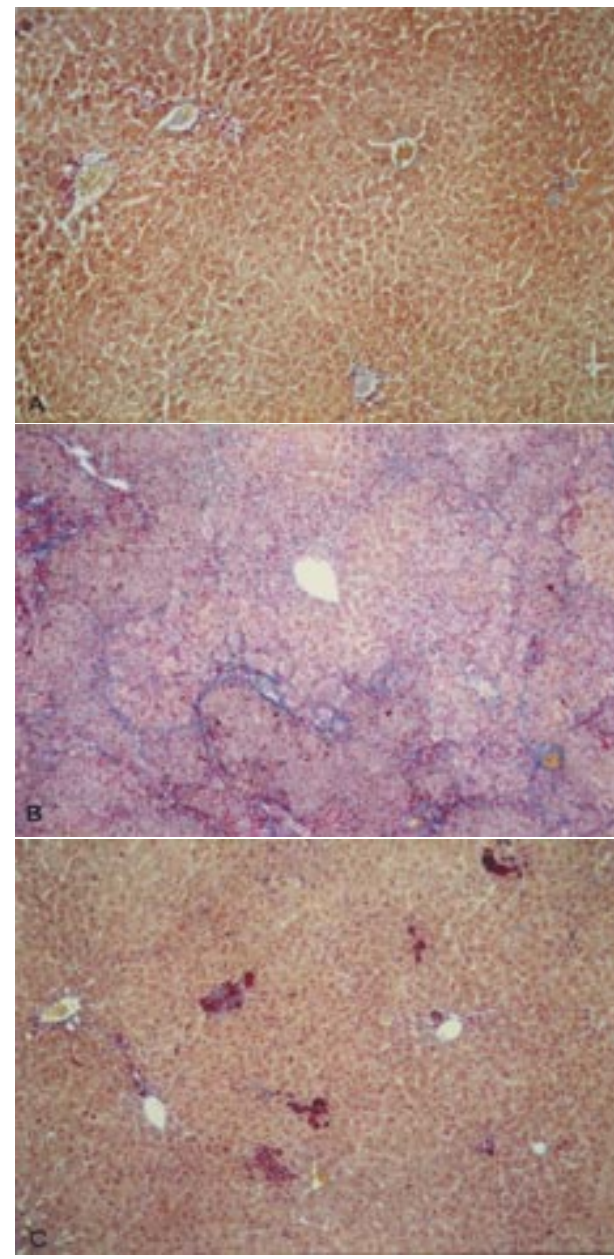

Fig. 1. Collagen accumulation in iron-treated gerbils. Liver sections from control (A), iron-treated (B), and iron-treated silybin-gavaged (C) gerbils were processed for Masson stain. Iron induced a dramatic accumulation of collagen with typical nodularity appearing after 8 weeks (B). Silbyin totally prevented fibrosis (C). Original magnification: (A), (B), (C) = 133X.

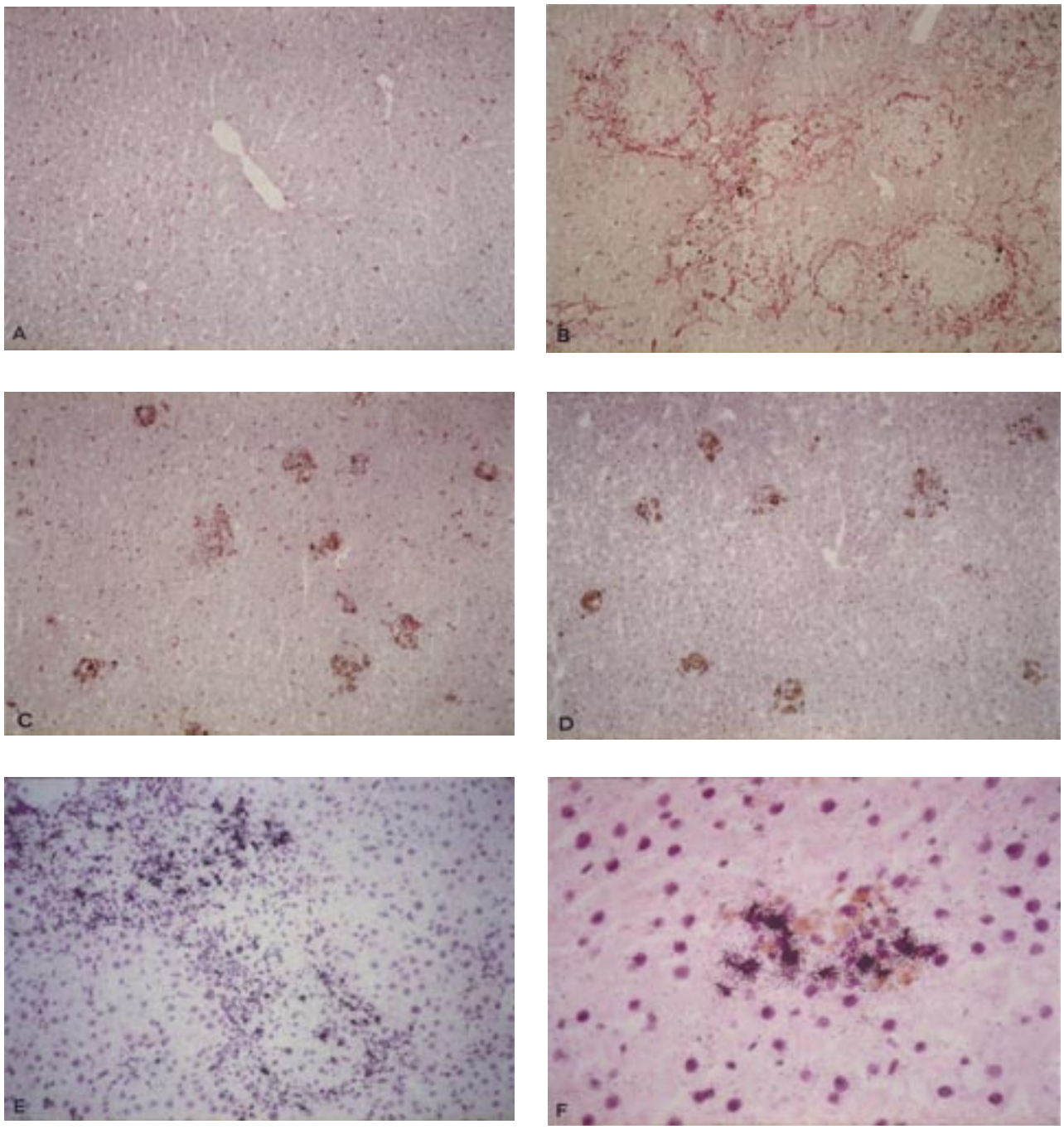

Fig. 2. Activation of hepatic stellate cells (HSC) in iron-treated gerbils. Liver sections from control (A), iron-treated (B, E), or iron-treated silybin-gavaged gerbils (C, D, and F) were processed for immunocytochemistry with monospecific antisera to desmin alone (A through D) or with in situ hybridization analysis with a specific collagen [^{35}S]-antisense cRNA probe (E and F). After iron treatment desmin positive cells dramatically proliferated and surrounded residual hepatocyte nodules (B). However, contemporary administration of silybin prevented espansion of HSC population (C). No specific signal was detected by using nonimmune sera (D). Seemingly, in iron-treated gerbils, a dramatic increase of collagen signal was detected (dark grains) (E), while silybin blocked activation showing only residual collagen activation in microfoci due to preexisting necrosis (F). Original magnification: (A), (B), (C), (D), (E) = 133X; (F) = 532X.

normal lobular architecture (Fig. 1(C)) and totally abolished HSC proliferation leaving a normal lobular structure with preexisting foci loaded with iron (yellowish spots) (Fig. 2(C)).

Iron Overload and Oxidative Stress

It is well-known that oxidant stress is responsible for enhanced fibrogenesis during experimental iron overload (Pietrangelo, 1996). To identify which hepatic cells were involved by oxidant-stress events during iron overload in the gerbil, liver sections were analyzed by in situ hybridization using a cRNA probe for HO-1, a stress-response gene specifically sensitive to cellular oxidative stress (Poss and Tonegawa, 1997). HO-1 mRNA signal was dramatically enhanced in nonparenchymal cells invading the large bundles of fibrous tissue, but spared nearby residual hepatocyte nodules (Fig. 3(B)). Yet, silybin treatment, appreciably decreased HO-1 expression which was confined to small preexisting necrotic foci (Fig. 3(D)). No specific hybridization signal was detected by using a HO-1 sense probe (Fig. 3(C)).

In order to assess whether lipid-peroxidation byproducts accumulated in iron-loaded cells, immunocytochemistry for malondialdehyde (MDA)–protein adducts was performed (Bedossa *et al.*, 1994). Diffuse immunostaining was specifically seen over large bundles of nonparenchymal cells and fibrous septa after 8 weeks of iron treatment (Fig. 4(B)) as compared with control gerbils (Fig. 4(A)), with no significant staining over hepatocytes. By using nonimmune serum, no immunoreactivity was detected (Fig. 4(C)). After silybin treatment MDA–protein adduct accumulation was restricted to small preexisting necrotic iron-foci (Fig. 4(D)).

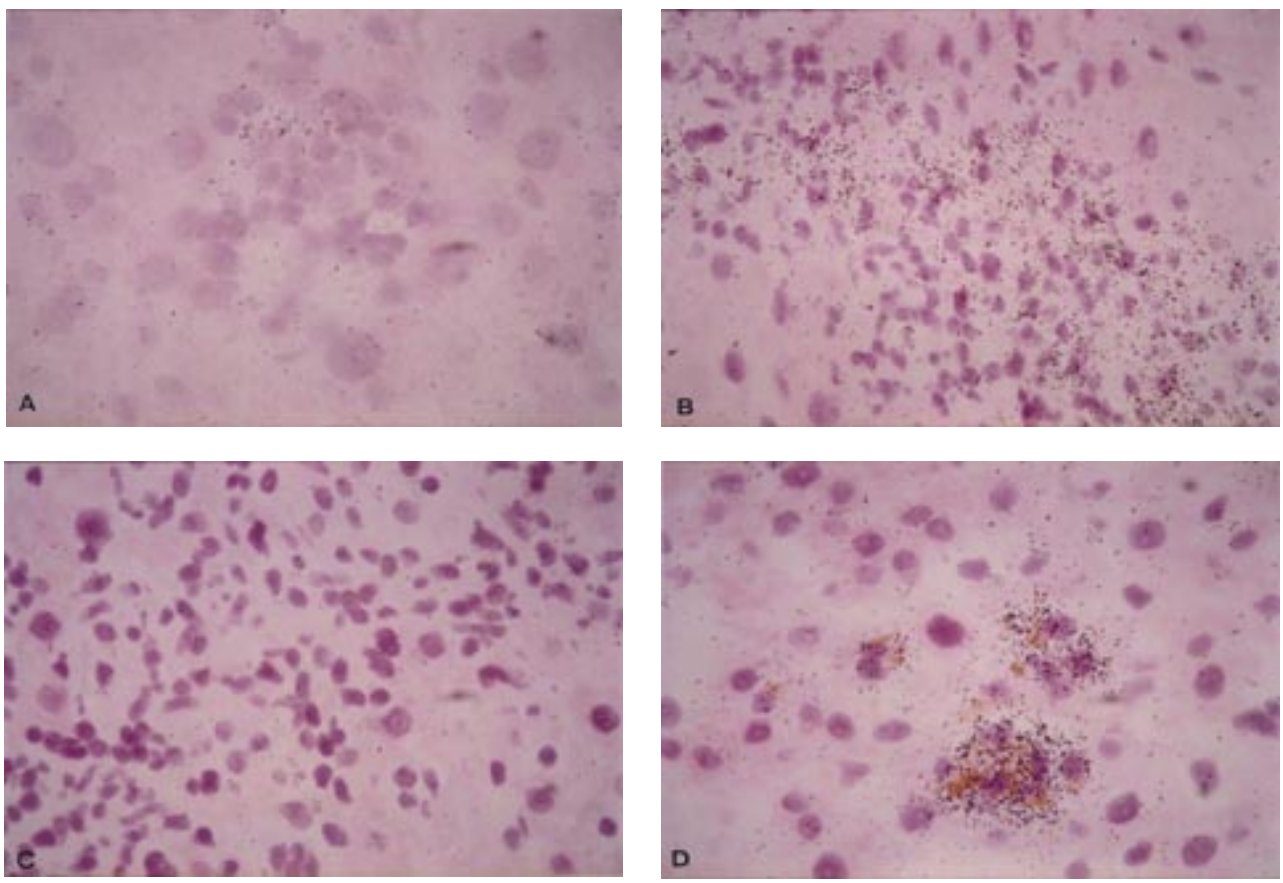

Fig. 3. Heme oxygenase-1 mRNA accumulation and HSC activation in iron-loaded gerbils. In situ hybridization analysis with a specific heme oxygenase-1 (HO-1) [^{35}S]-antisense (A, B, D) or sense (C) cRNA probe was performed on liver specimens from a control gerbil (A) or gerbils treated with iron (B and C) or iron plus silybin (D). HO-1 mRNA signal dramatically increased in nonparenchymal cells forming bundles of fibrous tissue, but spared the hepatocytes (B). No specific hybridization signal was detected by using a HO-1 sense probe (C). However, administration of silybin, dramatically decreased HO-1 expression which was limited to small iron-foci (D). Original magnification: (A) = 839X; (B), (C), (D) = 532X.

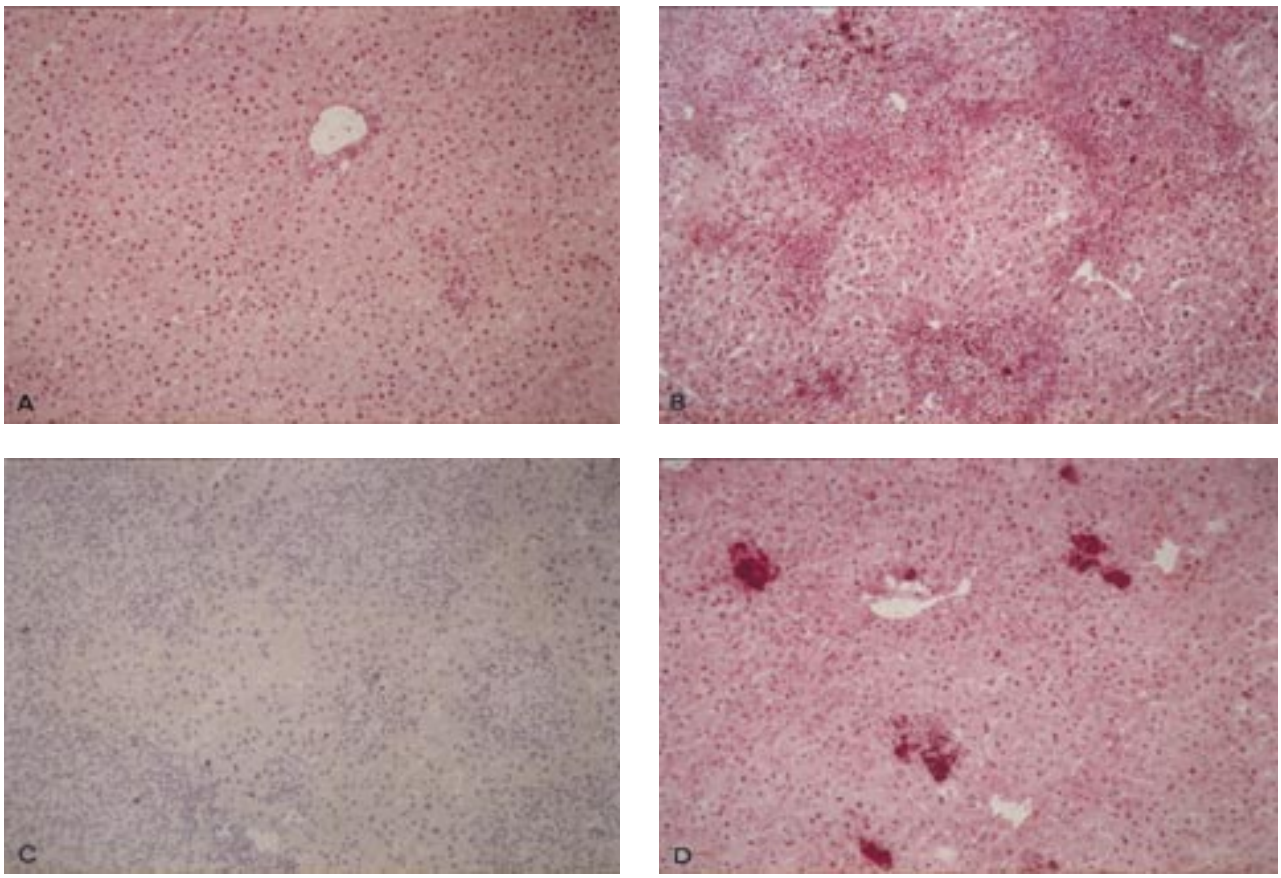

Fig. 4. Accumulation of malondialdehyde–lysine protein adducts in the liver of iron-loaded gerbils. Liver sections from control (A), iron-treated (B, C), or iron-treated silybin-gavaged gerbils (D) were processed for immunocytochemistry with monospecific antisera to malondialdehyde–lysine adducts alone as specified in Materials and Methods. Fig. 4(C) refers to liver section from iron-dosed gerbil processed with nonimmune sera. *Sections were counterstained with hematoxylin alone to visualize nuclei, while the slightly background is due to nonspecific polyclonal antibody section staining*. Immunostaining is specifically intense over large bundles of nonparenchymal cells and fibrous septa (B). In gerbils treated with iron plus silybin MDA–adduct signal was confined to small iron-filled foci (D). Original magnification: 133X.

Iron Overload and Mitochondrial Functional Integrity

A major role in generation of noxious reactive oxygen species (ROS) in the cell is now ascribed to the so-called "chelatable iron-pool" (Breuer *et al.*, 1995; Cabantchick *et al.*, 1996; Ferrali *et al.*, 1990). Mitochondria represent an important source of ROS in physiological and pathophysiological states (Fisher, 1987). We studied the effects of hepatic iron overload alone or in combination with silybin treatment on the level of this critical iron pool, on lipid peroxidation and on the energy transducing capability in isolated mitochondria.

The content of the DFO-chelatable iron pool largely increased upon iron intoxication and silybin administration fully prevented this increase (Table II). The same table shows that MDA content of mitochondrial membranes from siderotic gerbils was significantly greater than that from controls, and the combined silybin treatment appreciably prevented mitochondrial MDA accumulation following iron treatment.

Table II. Total Iron, Chelatable Iron, and TBARS in the Hepatic Mitochondrial Fraction From Iron-Treated Gerbils

Experimental condition	Total iron (nmol/mg protein)	Chelatable iron (pmol/mg protein)	TBARS (nmol/mg protein)
Control	33 ± 5	273 ± 38	0.187 ± 0.015
Iron	$276 \pm 18^*$	$530 \pm 41^*$	$0.392 \pm 0.025^*$
Silybin	38 ± 8	214 ± 42	0.190 ± 0.010
Iron + silybin	$282 \pm 26^*$	330 ± 36	0.215 ± 0.020

Note. Total iron, chelatable iron, and TBARS analyses were performed as described in Materials and Methods. Data are expressed as mean ± SD of three experiments performed on a pool of four animals.
$^*P < 0.01$ in comparison with control.

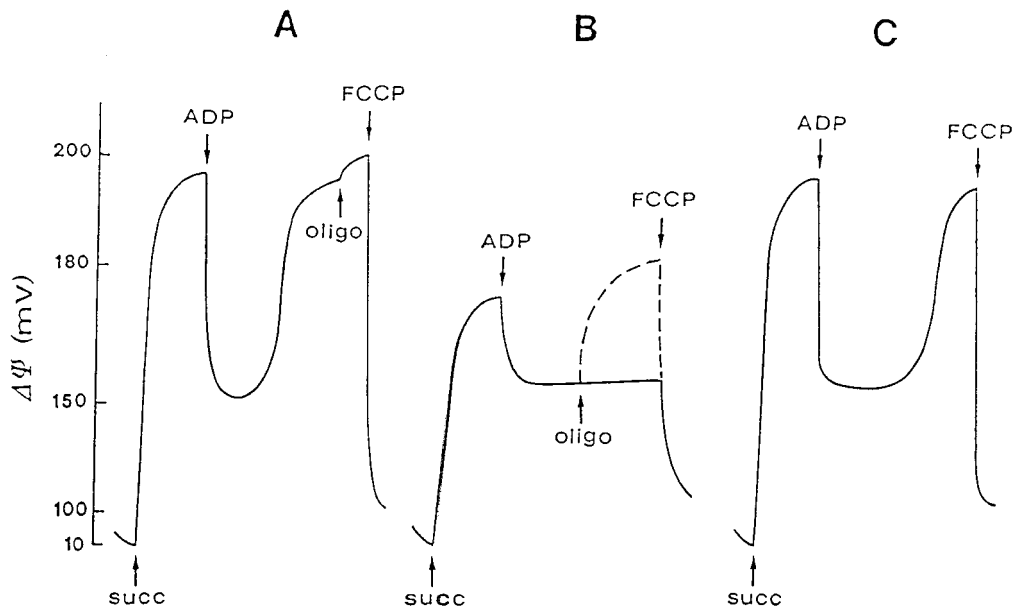

Fig. 5. Hepatic mitochondrial membrane potential during a complete cycle of phosphorylation in iron-overloaded gerbils. Mitochondria (2 mg/mL) in the standard incubatium medium were energized by the addition of 2 mmol/L succinate (succ). The arrows indicate the following addition: 0.25 mmol/L adenosine diphosphate (ADP), 0.2 μmol/L carbonyl cyanide-*p*-trifluoromethoxyphenylydrazone (FCCP), 2 μg/mg protein oligomycin (oligo). (A) control mitochondria; (B) mitochondria from iron-treated gerbils; (C) mitochondria from iron-treated, sylibin-administered gerbils. The mitochondrial membrane potential was measured by a tetraphenylphosphonium selective electrode as described in "Materials and Methods." The traces shown are representative of at least three different experiments performed on a pool of four animals.

The effect of hepatic iron overload alone or in combination with silybin treatment on mitochondrial functional efficiency was investigated by measuring the mitochondrial transmembrane electrical potential ($\Delta\Psi$). Figure 5(A) shows the membrane potential of liver mitochondria from control gerbils in different metabolic states. Mitochondria from iron-treated gerbils (Fig. 5(B)), in the presence of succinate (State 4) developed a maximum $\Delta\Psi$ of 175 mV, a value substantially lower than that of control (194 mV). Furthermore, the membrane potential, after the drop to 158 mV caused by ADP, remained at the decreased level. The subsequent addition of oligomycin, a specific inhibitor of respiration tightly coupled to phosphorylation (Masini *et al.*, 1983), immediately restored $\Delta\Psi$ to a value slightly higher than the pre-ADP level, i.e. 181 mV. On the contrary, the addition of either an antioxidant, such as BHT, or of an iron chelator, such as DFO, did not modify $\Delta\Psi$ trace. At this point, the addition of FCCP promptly collapsed $\Delta\Psi$. It is noteworthy that the respiratory rate of these mitochondria under the same metabolic conditions was in agreement with the membrane potential behavior (not shown). The contemporary administration of silybin to iron-treated gerbils largely prevented membrane potential anomalies, the only difference with control mitochondria being a longer time length to complete the phosphorylation cycle i.e. 5 min (Fig. 5(C)).

A significant reduction in the respiratory chain enzyme activities, i.e. NADH:cytochrome *c* reductase (complex I + III), succinate:cytochrome *c* reductase (complex II + III), cytochrome *c* oxidase (complex IV), and succinate dehydrogenase (complex II) resulted associated with iron treatment (Table III). The contemporary administration of silybin fully prevented the decrease in enzyme activities.

The functional integrity of cytochrome *c* oxidase depends on the presence of intact phospholipids, especially cardiolipin (Fry and Green, 1980). The presence or the absence in the standard reaction medium of lubrol, a nonionic detergent which facilitates the substrate accessibility, may give an insight into the structural integrity of the inner mitochondrial membrane (Muscatello and Carafoli, 1969). Iron administration to gerbils largely reduced the extent of lubrol activation of cytochrome *c* oxidase activity (14%) in freeze-thawed liver mitochondria in comparison with control (62%) (Fig. 6). The contemporary administration of silybin with iron largely restored the extent of lubrol activation (45%). Similar results were obtained for succinate dehydrogenase activity (not shown). On the

Table III. Enzyme Activities of the Respiratory Chain in the Hepatic Mitochondrial Fraction From Iron-Treated Gerbils

	Control	Iron	Silybin	Iron + silybin
NADH:cytochrome *c* reductase (nmol/(min mg protein))	139 ± 10	$106 \pm 9^*$	142 ± 13	132 ± 12
Succinate: cytochrome *c* reductase (nmol/(min mg protein))	204 ± 16	$159 \pm 15^*$	196 ± 14	186 ± 21
Cytochrome *c* oxidase (ng atom O/(min mg protein))	511 ± 37	$406 \pm 32^*$	481 ± 35	452 ± 38
Succinate dehydrogenase (ng atom O/(min mg protein))	94 ± 7	$69 \pm 6^*$	101 ± 8	80 ± 8

Note. Enzyme activities were measured as described in Materials and Methods. Data are expressed as mean ± SD of three experiments performed on a pool of four animals.
$^*P < 0.01$ in comparison with control.

other hand, the animal group treated with silybin alone, showed no difference from the control group, thus relevant data were not reported in the figure.

The mitochondrial functional derangement due to iron treatment, was found to be associated with a dramatic decrease in the hepatic ATP content, i.e. $0.78 + 0.16$ pmol/g wet weight in comparison with $1.98 + 0.11$ pmol/g wet weight of control, was detected in intoxicated gerbils (Fig. 7). Silybin administration fully prevented the ATP decrease. No difference from the control group was observed in the group treated with silybin alone, thus relevant data were not reported in the figure.

By electron microscopy marked structural alterations were detected in mitochondria of nonparenchymal cells, especially Kupffer cells, in iron dosed gerbils. These mitochondria presented matrix rarefaction, diffuse vacuolization, and swelling (Fig. 8(B)). By contrast, in the hepatocytes, mitochondria were apparently normal. Nevertheless, they showed increased amount of inner membranes and clustered cristae (Fig. 8(C)) as compared with controls (Fig. 8(A)).

DISCUSSION

In the present experimental model of acutely iron-dosed gerbil we observe a significant rise in the DFO-chelatable iron pool in the liver mitochondrial fraction. This appears to be responsible for the induction of oxidative stress associated with irreversible dysfunctions of mitochondrial oxidative metabolism and a marked reduction in the hepatic ATP level. By using in situ morphological and molecular biology approach, we show that such abnormalities specifically occurs in nonparenchymal

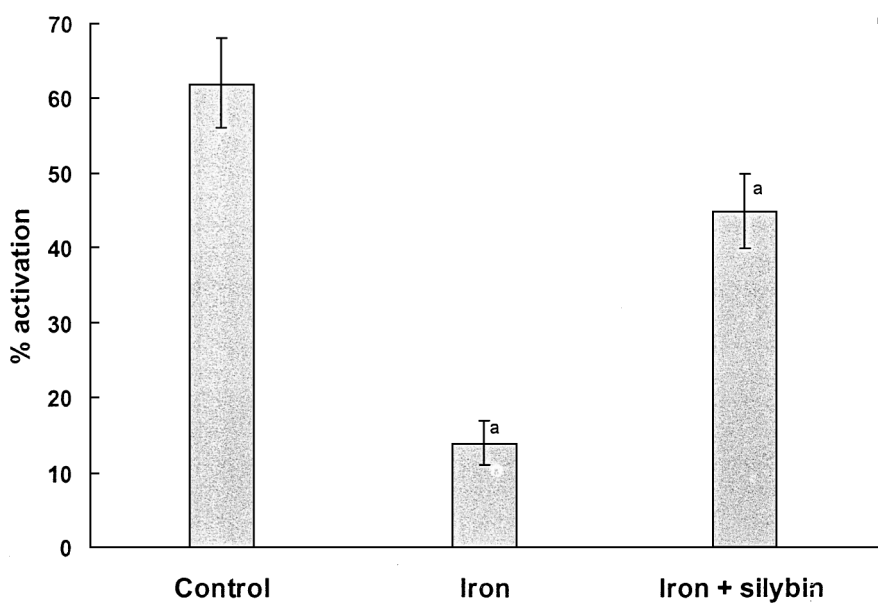

Fig. 6. Extent of lubrol activation of cytochrome *c* oxidase activity in various experimental groups. The percent changes from the values of enzyme activity measured in the absence of lubrol in the reaction medium are shown. All other conditions as in Table III. $P < 0.01$ in comparison with control.

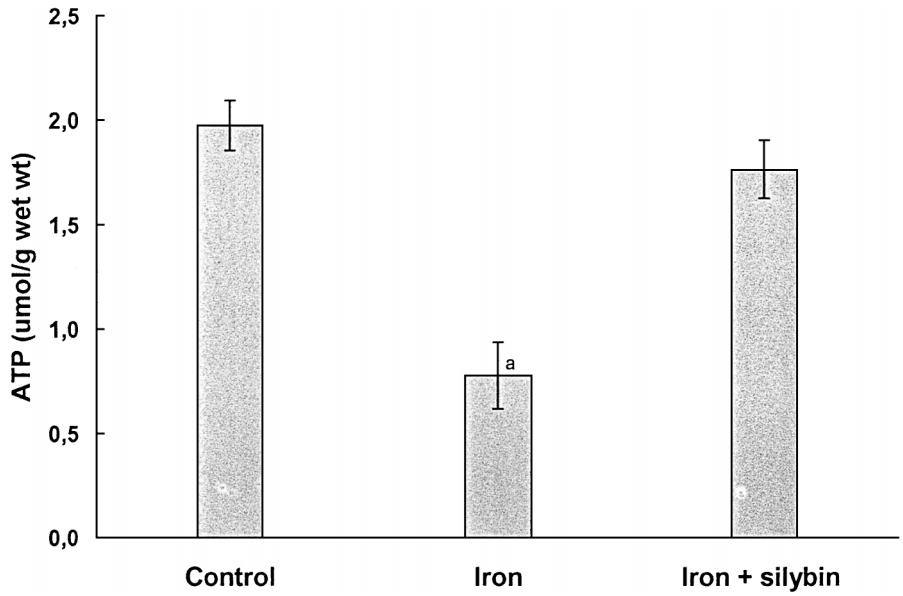

Fig. 7. Adenosine triphosphate level in the hepatic tissue of iron treated gerbils. Adenosine triphosphate analysis was performed as described in Materials and Methods. Data are expressed as mean ± SD of three experiments performed on a pool of four animals. $P < 0.01$ in comparison with control.

hepatic cells where iron primarily accumulates. By hindering the increase of DFO-chelatable iron level through the oral administration of a potent antioxidant such as silybin, the oxidative-stress induced mitochondrial derangement, the expansion of nonparenchymal cell population and fibrogenesis are prevented.

The enhancement of lipid peroxidation in mitochondria appears to be dependent on the increase of the catalitically active DFO-chelatable iron pool. The observation that the protective action of silybin against iron-induced oxidative injury strictly depends on its capability to counteract the rising of mitochondrial chelatable iron level, in spite of unchanged total liver iron burden, gives experimental support to the above conclusion. In fact, in this model of acutely iron-treated gerbil where the level of mitochondrial DFO-chelatable iron is 530 ± 41 pmol/mg protein, the silybin treatment makes the DFO-chelatable iron level to be quite similar to control. In a previous study on chronically iron-dosed gerbil where the DFO-chelatable iron in mitochondria was found to be 2482 ± 220 pmol/mg protein, the silybin treatment was not able to fully counteract the rising of this iron pool which remained at a value of 1588 ± 160 pmol/mg protein (Masini *et al.*, 2000). As a consequence, the silybin administration only partially prevented the iron-induced oxidative stress and the associated functional abnormalities. The above considerations and the observation that the extent of the functional derangement was much higher in the chronic treatment (Masini *et al.*, 2000), indicate the occurrence of a correlation between the level of DFO-chelatable iron and the extent of functional impairment. These results also indicate that the well-known "antioxidant" activity of silybin, and possibly of other flavonoids, may be due to a "primary" antioxidant effect consisting in iron chelation, as supported by recent data (Ferrali *et al.*, 1997).

One aspect which deserves further considerations is the mitochondrial fraction that has been utilized in the study. Liver mitochondria have been isolated by differential centrifugation and unavoidably present some contaminant lysosomes. Iron-loaded lysosomes could be misleading (Tangeras, 1983) for the interpretation of the present results; indeed, iron released from the lysosomal compartment during sample preparation could cause or contribute to the structural and functional impairment of mitochondria. However, this possibility has been completely ruled out in previous studies where the same methodological approach of this present study was adopted (Bacon *et al.*, 1985; Masini *et al.*, 1989).

It is worthy to note that the mitochondrial fraction utilized for functional studies has been derived from whole liver, an organ physiologically composed of cells that differ in structure and function. In fact, we find marked structural alterations only in mitochondria of Kupffer cells. Mitochondria of hepatocytes, on the contrary, apparently normal, show morphological aspects which are characteristics of an adaptive process correlated to the oxidative stress. The actual value of membrane

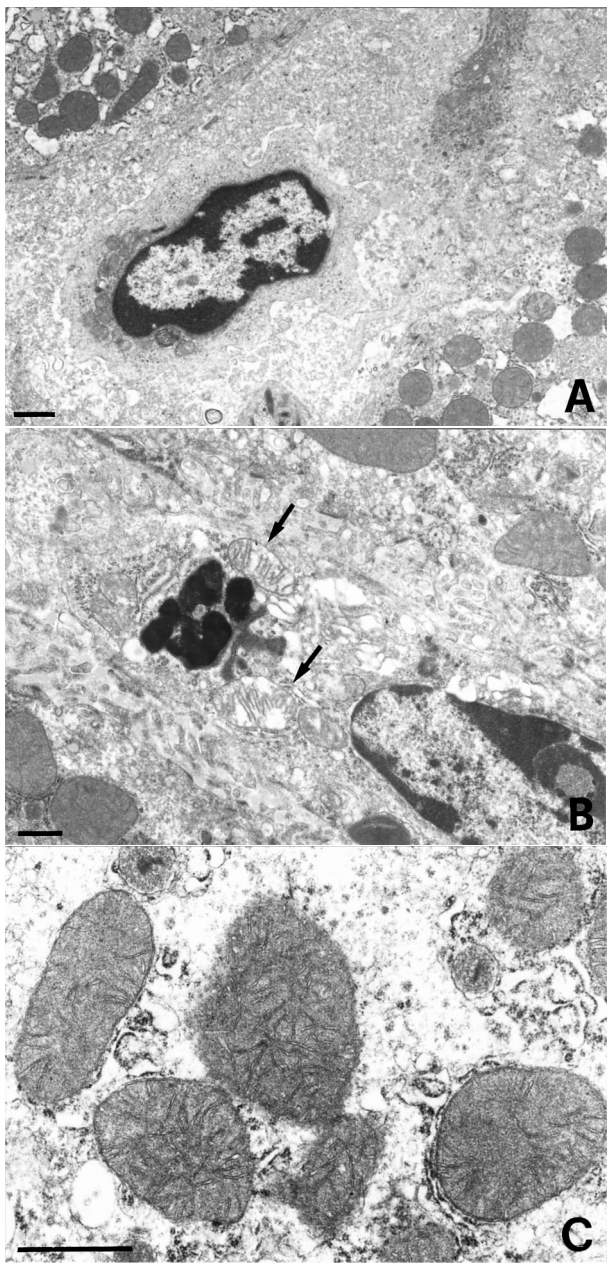

Fig. 8. Mitochondrial morphology in nonparenchymal cells and hepatocytes of control and iron-treated gerbils. The micrographs show altered mitochondria (arrows) in a nonparenchymal cell (B) and adapted mitochondria in an hepatocyte of iron-treated gerbil (C) as compared with control (A). *Black spots are iron particles*. Bar $= 1\ \mu$.

potential measured results, in fact, from the average of opposite functional modifications.

Mitochondria play a primary role within the cell both in the handling of iron and in energy production by oxidative phosphorylation process. They represent a primary target of oxidative injury, and at the same time they are the main source for reactive oxygen species (ROS). In fact, ROS are produced through the respiratory chain at a rate which is dependent on the metabolic state (Chance *et al.*, 1979). In the presence of iron ions, ROS give rise to highly-reactive oxidizing species (OH and reactive iron–oxygen radicals) (Boveris and Chance, 1973; Cadenas *et al.*, 1977; Chance *et al.*, 1979; Erencinska and Wilson, 1982; Halliwell and Gutteridge, 1988; Nohl and Hegner, 1978). The destabilization of one or more components of the electron transport chain (Dryer *et al.*, 1980) leads to an increased production of ROS. Since these two conditions occur in nonparenchymal cell mitochondria this results in an overproduction of ROS. ROS may exert mitogenic and chemoattractant effects on nonparenchymal cells (Perez *et al.*, 1980). In the iron-treated gerbils, iron load, oxidant-stress gene response, and lipid peroxidation by-products have been found in nonparenchymal liver cells where also mitochondrial alterations have been localized y ultrastructural studies. In fact, ROS generation is known also to occur during activation of Kupffer cells and of invading neutrophyls through membrane-bound NADPH oxidase (the so called "oxidative burst") in the same nonparenchymal cell population. In the gerbil, gut endotoxins are likely to be responsible for the microscopic necro-inflammatory foci seen in control animals (Carthew *et al.*, 1991). The latter, unless they are targeted with excess iron, do not expand and no signs of fibrosis are seen in the liver of control gerbils even after long time period (Carthew *et al.*, 1991; Pietrangelo *et al.*, 1995a). It can be suggested that selective iron load of these "primed" nonparenchymal cells including Kupffer cells dramatically enhances ROS generation and triggers fibrogenesis without inducing hepatocellular necrosis. In keeping with this hypothesis, a recent study has shown that iron targeting to "quiescent" Kupffer cells is unable to induce necrosis and fibrogenesis (Gualdi *et al.*, 1994). The fact that antioxidants are able to prevent liver fibrogenesis by blocking oxidative stress phenomena in these cells, indicates that ROS production in this cell population plays a key role for fibrogenesis. In fact, in an established model of oxidant-stress-related liver fibrogenesis (i.e. CCl_4 intoxication), we have recently found that oxidant stress activates HSC and fibrogenesis in paracrine fashion (Montosi *et al.*, 1998). Enhanced ROS generation may fuel oxidant-dependent pathways underlying cytokine production in inflammatory cells which accompanies active fibrogenesis. In fact, transcription factors like NF-kB and AP-1 involved in cytokine gene control, are modulated by the redox state of the cell (Sen and Packer, 1996). As to this point, it must be noted that activity of a potent fibrogenic cytokine, TGF-β, is also controlled by ROS production (Barcellos-Hoff and Dix, 1996). This same cytokine is dramatically

activated in iron-laden nonparenchymal cells in the gerbil (Pietrangelo *et al.*, 1995a).

In conclusion, our data indicate that iron functions as a potent profibrogenic factor when acting on a preinjured liver and, particularly, on preactivated nonparenchymal cells. Through an oxidative-stress-driven proinflammatory effect in the latter cell population, and in the absence of additional necrotic events, iron can dramatically enhance the drive to fibrosis and cirrhosis. The fact that the only experimental models in which liver cirrhosis has been obtained following iron treatment include iron-loaded animals treated with ethionine or low protein diet (Goldberg and Smith, 1955), iron-treated rats with CCl_4 alone (Kent *et al.*, 1964) or in combination with alcohol (Mackinnon *et al.*, 1955), and iron-treated rats with alcohol intoxication and high fat diet (Tsukamoto *et al.*, 1995), strongly support the cofactorial role of iron in fibrogenesis. *Our present data, although suggest on morphological grounds that mitochondrial derangement mainly involves nonparenchymal cells, cannot conclusively prove it. Attempts to isolate different hepatic cell populations and make evaluation of mitocondria in different cell isolates have failed due to massive lysis of iron-loaded cells during isolation procedure (A. P., personal communications). Therefore, we cannot rule out an alternative possibility: that hepatic iron accumulation damages hepatocyte mitochondria leading to inhibited electron transport chain activity, decreased oxidative phosphorylation, and increased ROS production; the latter might then trigger in a paracrine fashion fibrogenesis (Gualdi* et al., *1994). Nevertheless, regardless of the primary event, in the gerbil model of iron overload, oxidant stress in microinflammatory foci through mitochondrial derangement is clearly responsible for accelerated fibrogenesis*. The present experimental findings may have important implications for the comprehension of the pathogenesis of hepatic fibrosis where a synergism between endotoxin and iron occurs. Furthermore, the silybin properties described in the present study, suggest that a therapeutical approach targeted at decreasing the catalytically active iron pool in nonparenchymal cells may be extremely effective in preventing or controlling hepatic fibrogenesis.

ACKNOWLEDGMENTS

This work was supported by a grant "Progetti Avanzati" from the University of Modena and Reggio Emilia, Italy.

REFERENCES

Bacon, B. R., Park, C. H., Brittenham, G. M., O'Neill, R., and Tavill, A. S. (1985). *Hepatology* **5**, 789–797.

Barcellos-Hoff, M. H., and Dix, T. A. (1996). *Mol. Endocrinol*. **10**, 1077–1083.

Bedossa, P., Houglum, K., Trautwein, C., Holstege, A., and Chojkier, M. (1994). *Hepatology* **19**, 1262–1271.

Botti, B., Ceccarelli, D., Tomasi, A., Vannini, V., Muscatello, U., and Masini, A. (1989). *Biochim. Biophys. Acta* **992**, 327–332.

Boveris, A., and Chance, B. (1973). *Biochem. J*. **134**, 707–716.

Breuer, W., Epsztejn, S., and Cabantchik, Z. I. (1995). *J. Biol. Chem*. **270**, 24209–24215.

Cabantchik, Z. I., Glickstein, H., Milgram, P., and Breuer, W. (1996). *Anal. Biochem*. **233**, 221–227.

Cadenas, E., Boveris, A., Ragan, C. I., and Stoppani, A. O. M. (1977). *Arch. Biochem. Biophys*. **180**, 248–257.

Cairo, G., Tacchini, L., Schiaffonati, L., Rappocciolo, E., Ventura, E., and Pietrangelo, A. (1989). *Biochem. J*. **264**, 925–928.

Carthew, P., Edwards, R. E., Smith, A. G., Dorman, B., and Francis, J. E. (1991). *Hepatology* **13**, 534–539.

Chance, B., and Williams, G. R. (1956). *Adv. Enzymol*. **17**, 65–130.

Chance, B., Sies, H., and Boveris, A. (1979). *Physiol. Rev*. **59**, 527–605.

Dryer, S. E., Dryer, R. L., and Autor, A. P. (1980). *J. Biol. Chem*. **10**, 1054–1057.

Erecinska, M., and Wilson, D. F. (1982). *J. Membr. Biol*. **70**, 1–14.

Ferrali, M., Ciccoli, L., and Comporti, M. (1989). *Biochem. Pharmacol*. **38**, 1819–1825.

Ferrali, M., Ciccoli, L., Signorini, C., and Comporti, M. (1990). *Biochem. Pharmacol*. **40**, 1485–1490.

Ferrali, M., Signorini, C., Caciotti, B., Sugherini, L., Ciccoli, L., Giachetti, D., and Comporti, M. (1997). *FEBS Lett*. **416**, 123–129.

Fisher, A. B. (1987). In *Oxygen Radicals and Tissue Injury* (Halliwell, B., ed.), FASEB, Bethesda, MD, pp. 34–39.

Friedman, S. L. (1993). *N. Engl. J. Med*. **328**, 1828–1835.

Fry, M., and Green, D. E. (1980). *Biochem. Biophys. Res. Commun*. **93**, 1238–1246.

Genovese, C., Rowe, D., and Kream, B. (1984). *Biochemistry* **23**, 6210–6216.

Goldberg, L., and Smith, J. P. (1955). *Am. J. Clin. Pathol*. **25**, 514–542.

Gualdi, R., Casalgrandi, G., Montosi, G., Ventura, E., and Pietrangelo, A. (1994). *Gastroenterology* **107**, 1118–1124.

Halliwell, B., and Gutteridge, J. M. C. (1988). *ISI Atlas Sci. Biochem.* **1**, 48–52.

Hatefy, Y., and Stiggal, D. L. (1978). *Meth. Enzymol*. **53**, 5–10.

Houglum, K., Filip, M., Witztum, J. L., and Chojkier, M. (1990). *J. Clin. Invest*. **86**, 1991–1998.

Kamo, N., Muratsugu, M., Hongoh, R., and Kobatake, Y. (1979). *J. Membr. Biol*. **49**, 105–121.

Kent, G., Volini, F. I., and Minick, O. T. (1964). *Am. J. Pathol*. **45**, 129–155.

Kruck, T. P. A., Kalaw, W., Crapper, C., and McLachlan, D. R. (1985). *J. Chromatogr*. **341**, 123–130.

Mackinnon, M., Clayton, C., Plummer, J., Ahern, M., Cmielewski, P., Ilsley, A., and Hall, P. (1995). *Hepatology* **21**, 1083–1088.

Masini, A., Ceccarelli, D., Giovannini, F., Montosi, G., Garuti, C., and Pietrangelo, A. (2000). *J. Bioe. Biom*. **32**, 175–182.

Masini, A., Ceccarelli-Stanzani, D., and Muscatello, U. (1983). *FEBS Lett*. **160**, 137–140.

Masini, A., Ceccarelli, D., Trenti, T., Corongiu, F. P., and Muscatello, U. (1989). *Biochim. Biophys. Acta* **1014**, 133–140.

Montosi, G., Garuti, C., Iannone, A., and Pietrangelo, A. (1998). *Am. J. Pathol*. **1252**, 1319–1326.

Moreno, A. J. M., and Madeira, V. M. C. (1991). *Biochim. Biophys. Acta* **1060**, 166–174.

Muscatello, U., and Carafoli, E. (1969). *J. Cell. Biol*. **40**, 602–621.

Nohl, H., and Hegner, D. (1978). *Eur. J. Biochem*. **82**, 563–567.

Perez, H. D., Weksler, B. B., and Goldstein, I. A. (1980). *Inflammation* **4**, 313–328.

Pietrangelo, A. (1996). *Semin. Liver. Dis*. **16**, 13–30.

Pietrangelo, A., Borella, F., Casalgrandi, G., Montosi, G., Ceccarelli, D., Gallesi, D., Giovannini, F., and Masini, A. (1995c). *Gastroenterology* **109**, 1941–1949.

Pietrangelo, A., Casalgrandi, G., Quaglino, D., Gualdi, R., Conte, D., Milani, S., Montosi, G., Ventura, E., and Cairo, G. (1995b). *Gastroenterology* **108**, 208–217.

Pietrangelo, A., Gualdi, R., Casalgrandi, G., Montosi, G., and Ventura, E. (1995a). *J. Clin. Invest*. **95**, 1824–1831.

Poss, K. D., and Tonegawa, S. (1997). *Proc. Natl. Acad. Sci. U.S.A.* **94**, 10925–10930.

Sen, C. K., and Packer, L. (1996). *FASEB J*. **10**, 709–720.

Shibahara, S., Muller, R., Taguchi, H., and Yoshida, T. (1985). *Proc. Natl. Acad. Sci. U.S.A.* **82**, 7865–7869.

Tangeras, A. (1983). *Biochim. Biophys. Acta* **757**, 59–68.

Tisdale, H. D. (1967). *Methods Enzymol*. **10**, 213–215.

Tsukamoto, H., Horne, W., Kamimura, S., Niemela, O., Parkkila, S., Yla-Herttuala, S., and Brittenham, G. M. (1995). *J. Clin. Invest*. **96**, 620–630.

Weintraub, L. R., Goral, A., Grasso, J., Franzblau, C., Sullivan, A., and Sullivan S. (1988). *Ann. N.Y. Acad. Sci*. **526**, 179–184.